Neural Computing and Applications (2020) 32:2267–2281
https://doi.org/10.1007/s00521-018-3754-0

ORIGINAL ARTICLE

Iris tissue recognition based on GLDM feature extraction and hybrid MLPNN-ICA classifier

Neda Ahmadi[1] · Gholamreza Akbarizadeh[2]

Received: 21 June 2017 / Accepted: 26 September 2018 / Published online: 4 October 2018

Abstract
The use of iris tissue for identification is an accurate and reliable system for identifying people. This method consists of four main processing stages, namely segmentation, normalization, feature extraction, and matching. In this study, a new method of feature extraction and classification based on gray-level difference method and hybrid MLPNN-ICA classifier is proposed. For experimental results, our study is implemented on CASIA-Iris V3 dataset and UCI machine learning repository datasets.

Keywords Iris tissue recognition · Feature extraction · GLDM · Imperialist competitive algorithm · Multi-layer perceptron neural network

1 Introduction

Nowadays, people identification system from the iris tissue is the most accurate and reliable way of identifying individuals [1]. The human iris tissue is a complex structure with a lot of information in its texture that helps to perform the identification of each individual. Iris tissue is completed in fetal period and in the early years of birth and then remains unchanged until the end of the human's life. Iris tissue is an internal tissue that is protected and isolated from the outside environment; hence, there are a few environmental effects on it. Moreover, it is also available from outside and can be easily imaged from it. With these features, iris tissue became significant for researchers as an appropriate pattern for identification [2].

Classification and identification system, with respect to the iris tissue properties, can be divided into four general parts of segmentation, normalization, extracting unique features, and classification of iris patterns [3]. Several studies have been carried out on iris recognition systems, and various methods have been provided for segmentation and extraction of iris tissue characteristics [4–7]. Table 1 shows the list of acronyms.

The remainder of this paper is organized as below. Section 2 presents the problem description and our contribution. Section 3 reviews related and background work. Section 4 describes the preliminaries. Proposed method is introduced in Sect. 5. The experimental results are presented in Sect. 6, and the conclusion is given in Sect. 7.

2 Problem description and our contribution

With studying the existing studies in this field, we have found that the previous studies often used four fundamental steps including (1) iris tissue image acquisition (for enrollment and authentication stage), (2) iris tissue image localization and iris tissue normalization (for preprocessing stages), (3) feature extraction stage, and (4) pattern matching stage (in order to classify and detect iris tissue). At each step of this process, there are several methods that used. Selection of each of the methods in each step was done optionally. Although all techniques have certainly contributed to improving the latest scientific advances in the field of detecting iris tissue, there are still a number of

✉ Gholamreza Akbarizadeh
g.akbari@scu.ac.ir

[1] Department of Computer Engineering, Faculty of Engineering, Shahid Chamran University of Ahvaz, Ahvaz, Iran

[2] Department of Electrical Engineering, Faculty of Engineering, Shahid Chamran University of Ahvaz, Ahvaz, Iran

Table 1 List of acronyms

Acronyms	Description
ANN	Artificial neural network
GMM	Gaussian mixture model
SIFT	Scale-invariant feature transform
NSCT	Non-subsampled contourlet transform
GLDM	Gray-level difference method
GLCM	Gray-level co-occurrence matrix
SVM	Support vector machine
NS	Navier–Stokes
PB	Probable boundary
POC	Phase-only correlation
ACO	Ant colony optimization
PSO	Particle swarm optimization
SA	Simulated annealing algorithms
GA	Genetic algorithm
TA	Tabu search algorithm
HBMO	Honey bee matching optimization algorithm
CMC	Cumulative match scores characteristic
ICA	Imperialist competitive algorithm
PDF	Probability density functions
CHTA	Circular Hough transform algorithm
PB	Probable boundary
ROC	Receiver operating characteristic
FAR	False accept rate
FRR	False reject rate
GAR	Genuine accepted ratio

aspects that need improvement which is the practical application of the proposed algorithms. Many of the previous methods are very complicated. For example, the algorithm presented in [8] has high computational complexity due to the use of probabilistic neural network lonely in their proposed method; therefore, this algorithm is very time-consuming and expensive.

Thus, it can be said that so far different methods have been proposed to recognize the iris tissue that suffers from long run times, computational complexity, and high memory consumption; so, choosing a method that can accurately detect the iris tissue is a necessary issue. In this paper, by using the gray-level difference method (GLDM) feature extractor to extract the iris tissue and using the MLPNN-ICA for classifying purpose, we realize that the proposed algorithm while having less computational complexity can extract the iris tissue images with perfect accuracy rate and finally, it recognizes them with quit high rate 99.99%.

The contribution of the present study is to develop an efficient algorithm for the iris tissue in order to get high accuracy rate in the iris recognition system. The proposed algorithm is a combination of an efficient GLDM feature extraction technique for extracting the iris tissue features, and hybrid MLPNN-ICA classifier for classification of the iris tissue images.

In this paper, we look at the following key questions:

- How can the accuracy rate of the iris tissue images in the iris recognition system be improved?
- Does the robustness of combination of MLPNN and ICA classifiers and GLDM feature extraction impact on the iris tissue recognition accuracy?

To answer above questions, in this research, we apply GLDM to extract precise features from human iris tissue image and achieve better accuracy rate; then, a novel hybrid model based on hybrid MLPNN-ICA classifier is developed in order to distinguish the iris tissue images of different people. According to the experimental evaluations of our method, it can be seen that our proposed methodology is quite effective, low cost and obtains exact results in classification step for the iris tissue recognition system and there are no previous applications of united MLPNN and ICA algorithms for the iris tissue recognition problem.

3 Related and background work

In Othman et al. [9], a new iris recognition method for solving the low-quality iris recognition system was presented. They employed two quality measures that computed globally and locally, which were derived from GMM probabilistic characterization of iris image. Moroti and Munaga [10] conducted the iris segmentation method for solving eyelashes and eyelids problem. They employed adaptive thresholding and circular Hough transform for pupil boundary, and drew different radius arcs from the pupil center as well as discovering the highest change in intensity for iris boundary. Subsequently, they used scale-invariant feature transform (SIFT) for feature extraction step. In Khalighi et al. [11], the new feature extraction approach was developed based on new scale, shift and rotation invariant in both time and spatial frequencies. Then, a two-level non-subsampled contourlet transform (NSCT) was conducted on the iris images normalization, and calculated as a gray-level co-occurrence matrix (GLCM) in three various orientations on spatial image and NSCT frequency sub-bands. Atul et al. [12] developed a method for determining diabetes from iris recognition system based on support vector machine (SVM). They used 2-D wavelet tree for feature extraction step. Ning et al. [13] presented an iris recognition approach for noisy images that uses inpainting method based on Navier–Stokes (NS) equations, and for identifying pupil edge, probable

boundary (Pb) edge detection operator was used. Then, 1-D Log-Gabor filter was carried out for feature encoding step.

In Abiyev and Altunkaya [14], they presented an iris recognition system based on neural network that was trained by adaptive learning strategy and they carried out fast algorithm in order to localize the iris region. Cho and Kim [15] proposed 2-D wavelet transform based on Haar wavelet for feature extraction step, and they conducted a novel approach for determining winner in LVQ neural network. In Sundaram and Dhara [16], the new iris recognition method was developed for GLCM-based Haralick features. Thereafter, probabilistic neural network (PNN) was performed for matching process. Jain and Verma [17] proposed a new approach, based on phase-only correlation (POC) and neural network for recognition time, the rate of false detection, conditioning time, complexity of the algorithm, bulk detection, and database handling. In Atashpaz-Gargari and Lucas [18], imperialist competitive algorithm (ICA) which is one of the popular algorithms was used. In Niknam et al. [19], a novel method was introduced based on k-means and ICA that outcome overweighed than ACO, PSO, SA, GA, TA, and HBMO algorithms. Semi-supervised classification techniques can also be used for recognition of iris tissue. These techniques are useful when we have a limited amount of labeled data but many unlabeled samples [20, 21]. Qian et al. [20] proposed a semi-supervised classification with extensive knowledge exploitation, named as SSC-EKE. The main feature of the SSC-EKE method is the systematic incorporation of the tasks in which the connotation of extensive knowledge exploitation is embodied. But, the need to develop practicable methodologies for prompt and self-adaptive parameter setting in SSC-EKE is the challenges that should facilitate its applicability to real-world problems. Belkin et al. [21] proposed a family of learning algorithms based on a form of regularization that allows us to exploit the geometry of the marginal distribution. It was based on a representer theorem that provided a basis for several algorithms for unsupervised, semi-supervised and fully supervised learning. But, more systematic procedures need to be developed to choose the appropriate values for the extrinsic and intrinsic regularization parameters.

4 Preliminaries

4.1 Iris tissue image preprocessing

In order to obtain precise results in the iris tissue identification, we need to select the iris tissue images that have high quality; so, for this aim, the preprocessing steps were performed including two crucial steps: (1) the iris tissue localization and (2) the iris tissue normalization. These processes are very important to get an optimum region for the iris tissue recognition system. Usually, these processes have been employed on the acquired iris tissue images in order to achieve the ROI of iris tissue and also to diminish the iris image noises [22].

The first step of the preprocessing steps is the iris tissue localization. Since it is considered as an imperative step, it should be carried out superbly. In this step, inner and outer borders of the iris tissue are detected and after that the iris tissue sclera and pupil are separated from each other. Various techniques have been used for this purpose, and in our work, we utilized circular Hough transform algorithm (CHTA) [23, 24]. In the next step, for normalizing the iris tissue, we utilized the rubber-sheet model of Daugman [25, 26] which transforms the iris tissue image from the Cartesian coordinate space to polar coordinate space.

4.2 Gray-level difference method (GLDM)

This method [27] is based on two pixels that an absolute difference was given in the gray level and was separated by a specific displacement δ. Motion vector is defined in Eq. (1) and the probability density function is defined in Eq. (2):

$$\delta = (\Delta x, \Delta y) \quad \text{let} \quad S_\delta(x, y) = |S(x, y) - S(x + \Delta x, y + \Delta y)| \tag{1}$$

$$D(i|\delta) = \text{Prob}[S_\delta(x, y) = i] \tag{2}$$

which $\Delta x, \Delta y$ are the parameters of the method and they are integers, $S_\delta(x, y)$ is the input image, x and y are positions in image $S_\delta(x, y)$ with $1 \leq x \leq M$ and $1 \leq y \leq N$ (that M and N are the image dimensions). Then, by concatenating of contrast, angular second moment, entropy, and mean that are calculated from PDF, a feature vector is calculated.

4.3 Artificial neural networks and multi-layer perceptron (MLP)

The ANNs are one of the smart and universal computational algorithms which comprise a number of neurons in order to solve problems specifically. These systems are programmed for a special application by a learning procedure; for example, classification of data and pattern recognition. This process involves adjustment for connecting the synapses (which are among the neurons and these connections make a structure hierarchically) [28]. In order to classify non-separable problems, it needs to utilize more layers because the single layer perceptron has the ability to separate linearly problems [29]. In the network with one layer, just output layer is counted, but in the network with more layers, the hidden and output layers are counted and the layers in input are not counted as the

Table 2 Training MLPNN classifier

(1) Selecting training patterns for learning network
(2) Defining N input, $N-1$ hidden layers, and N output that must be fully connected layers with their prior layers by weigh of connection
(3) Producing initial weight randomly
(4) Choosing the error function $E(w)$ and η correctly
(5) Performing the updated weight to all weights (w) and all training patterns (p) $\Delta w = -\eta \partial E(w)/\partial w$
(6) Reiterating step 5, till the error function of network become adequately small

nodes, and also there is no need to calculate. In order to learn MLPNN, the network weights (w) are defined for minimizing the function of output cost which is the final layer output and shown in the output from error function E. The parameters η and p are learning rate and training pattern, respectively; so, learning MLPNN and updated weights by using gradient descent sets are defined in Eqs. (3, 4) [30].

$$E_{\mathrm{SSE}} = \frac{1}{2}\sum_{p}\sum_{j}\left(t\arg_j^p - \mathrm{out}_j^{(N)p}\right)^2 \tag{3}$$

$$\Delta w = -\eta\frac{\partial E(w)}{\partial w} \tag{4}$$

The training of the MLPNN algorithm as shown in Table 2 includes the following steps:

4.4 Imperialist competitive algorithm (ICA)

This algorithm is a method in the evolutionary computation area that finds optimal response of the different optimization problems. It also presents a technique for solving optimization mathematical problems, by mathematical modeling of social-political evolutionary process [18]. In terms of usage, this algorithm exists within the evolutionary optimization algorithms such as GA, PSO, ACO, SA, and so on. Like all other algorithms in this category, colonial competitive algorithm also makes up the basic set of possible solutions. The initial results in GAs are known as "chromosome", in the PSO algorithm, they are known as "particle" and in the ICA, they are known as "country". ICA with a special process that follows gradually improves the basic answers (countries) and eventually provides suitable response of optimization problem (desirable country). The main pillars of this algorithm form an assimilation policy, revolution, and colonial competition. This algorithm presents operators in the regular form by emulating social, economic, and political evolutionary process of countries, and by mathematical modeling of parts of this process, which can help to solve the complex optimization problems. Literally, this algorithm observes optimization problem answers in the nations form, and tries to improve these answers gradually in an iterative process and eventually leads to the optimal solution.

1. Shaping the early empires

In optimization, the aim is to discover an optimal solution, in terms of the problem variables. This algorithm creates an array of problem variables that must be optimized and this array is known as a country. In an optimization problem with N_{var} dimension, the length of an array is $N_{\mathrm{var}} \times 1$ and this array is defined by Eq. (5):

$$\mathrm{Country} = [p_1, p_2, \ldots, p_{N\,\mathrm{var}}] \tag{5}$$

Values of variables in a country are displayed in decimal numbers and the cost of each country is in the cost function of $f(p_1, p_2, \ldots, p_{N\,\mathrm{var}})$ which is defined by Eq. (6):

$$\mathrm{Cost} = f(\mathrm{country}) = f(p_1, p_2, \ldots, p_{N\mathrm{var}}) \tag{6}$$

From the perspective of cultural history, the constituent parts of a country can be considered as the country's sociopolitical characteristics, such as culture, language, economic structure, and other features. The normalized cost of an empire is defined by Eq. (7):

$$C_n = c_n - \max\{c_i\} \tag{7}$$

where c_n is the nth cost of the empire, and C_n is the normalized cost. With the normalized cost of all empires, normalized power of each empire is defined by Eq. (8):

$$P_n = \left|\frac{C_n}{\sum_{i=1}^{N_{\mathrm{imp}}} C_i}\right| \tag{8}$$

From another point of view, the normalized power of an empire is colonial ratio which is mandatory of the empire. The initial number of colonies for an empire is defined by Eq. (9):

$$\mathrm{N.C.}_n = \mathrm{round}\{p_n \cdot N_{\mathrm{col}}\} \tag{9}$$

where $\mathrm{N.C.}_n$ is the initial number of colonies of nth empire and N_{col} is the number of all of the colonies. To start the algorithm, we used N_{country} as the number of initial countries, and chose N_{imp} of the best members of the population (the countries with the lowest cost function value), as imperialists. The rest of N_{col} countries forming the colonies belong to an empire. To divide initial colonies between imperialists, the number of colonies was given to each of the imperialists, and this number is proportional to its

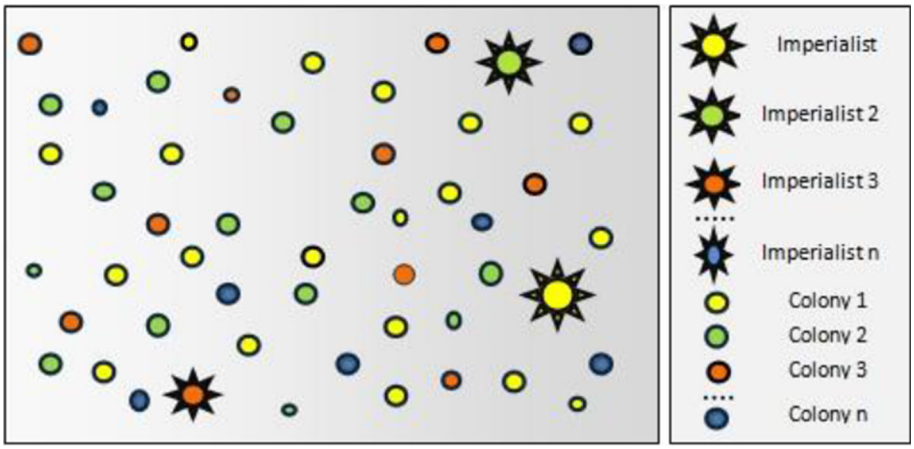

Fig. 1 How to divide colonies among colonial countries

power. Figure 1 shows how to divide the colonies between colonial countries symbolically.

2. The policy of assimilation: the colonies movement to the imperialist

The aim of analyzing the social structure and culture of the colonies in the central government culture is policy of assimilation (absorption). In order to increase the influence of the colonial countries, they began to create civil infrastructures (such as transportation infrastructure, university, etc.). For instance, countries such as Britain and France are thought to create New England and New France in their colonies by pursuing the policy of assimilation in their colonies. Literally, this central government has tried to attract the colonial country in line with different social-political dimensions, through the policy of assimilation, taking into account a country's way to solve the optimization problem. This part of the colonization process in the optimization algorithm was modeled as the colonies movement to the imperialist country. With this policy, the colony country moves to the imperialist in the direction of the colony line with x unit, and was drawn to the new position of the colony. X is the random number with uniform distribution (or any other suitable distribution). The distance between the imperialist is indicated by d and is defined by Eq. (10):

$$X \sim U(0, \beta * d) \tag{10}$$

where β represents a number that is greater than one and nearly equal to 2 (a suitable choice is $\beta = 2$). The coefficient of $\beta \geq 1$ makes the colony country moves to the imperialist country from different directions. In addition to this move, a small angular deviation is also added to the movement route with uniform distribution. A graphical view of the policy of assimilation in colonial competitive algorithm is illustrated in Fig. 2.

3. Revolution: a sudden change in the position of a country

Revolution creates sudden changes in the sociopolitical characteristics of a country. In ICA, revolution is modeled by random displacement of a colony country to a new random position. The algorithmic revolution implies that the evolutionary totality movement saves from stammer in the optimality local valleys which in some cases, improve the position of a country and take it to a better efficiency range.

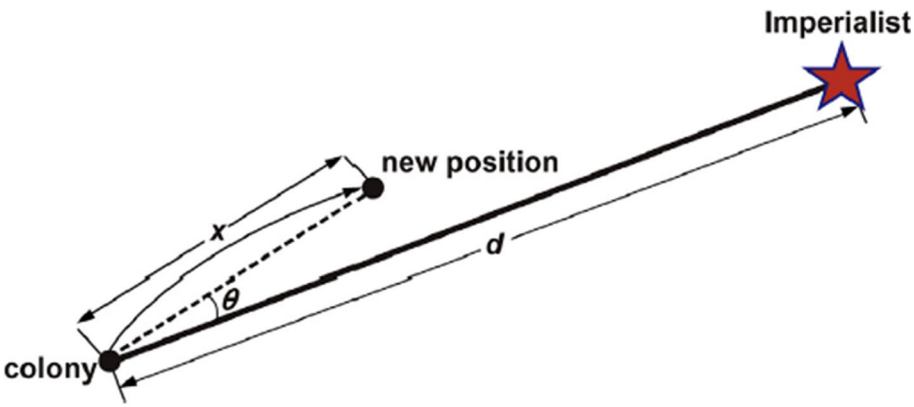

Fig. 2 Absorption policy in colonial competitive algorithm

4. The displacement position of the colony and imperialist

During the movement of colonies to the imperialist country, some of these colonies may attain a better position than imperialist (they may attain the points in the cost function that produces lower cost to the value of the cost function in the imperialist position). The colony and the imperialist countries change their place with each other. Furthermore, the algorithm is continued with the imperialist country in the new position and this time, the new imperialist country began to apply the policy of assimilation to their colonies. The placement of the colony and imperialist positions is illustrated in Fig. 3.

5. Colonial competition

The power of an empire is defined as a power of an imperialist country, in addition to a percentage of the total power of the colonies. Every empire that fails to increase its power and loses its competitiveness power is eliminated from the imperialist competitions. This removal is done gradually. This implies that weak empires lose their colonies over time and stronger empires conquer these colonies and enhance their power. In colonial competitive algorithm, the removing empire is the weakest empire. Thus, in algorithm iteration, one or more of the weakest colonies take the weakest empire, and in order to conquer these colonies, there is competition between all empires. The mentioned colonies are not necessarily conquered by the most powerful empire, but stronger empires may be more conquered. The total cost is defined by Eq. (11):

$$\begin{aligned} \text{T.C.}_n = {} & \text{Cost}(\text{imperialist}_n) \\ & + \xi \ \text{mean}\{\text{Cost}(\text{colonies of empire}_n)\} \end{aligned} \tag{11}$$

where T.C._n is the cost of nth empire, and ξ is a positive number less than 1. Small amounts of ξ show that the overall power of the empire is determined by the imperialists, while it enhances the colonies role in determining the overall power of an empire. Figure 4 shows the colonial competition between several imperialists and the overall normalized cost is defined by Eq. (12):

$$\text{N.T.C.}_n = \text{T.C.}_n - \max\{\text{T.C.}_i\} \tag{12}$$

where T.C._n and N.T.C._n are total cost and total normalized cost of the nth empire, respectively. With an overall

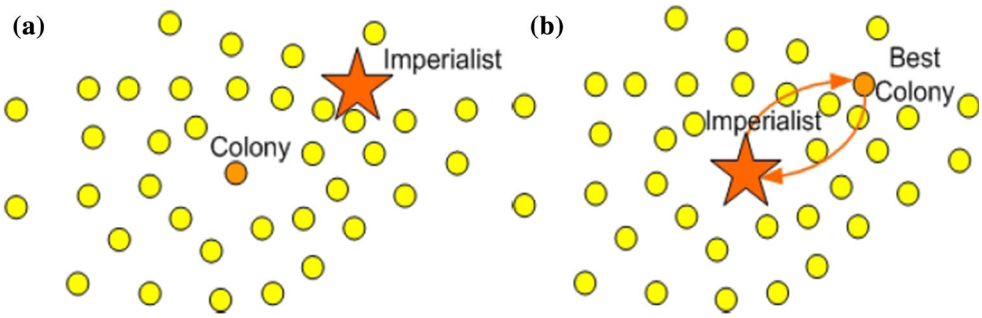

Fig. 3 Position displacement of colony and imperialist

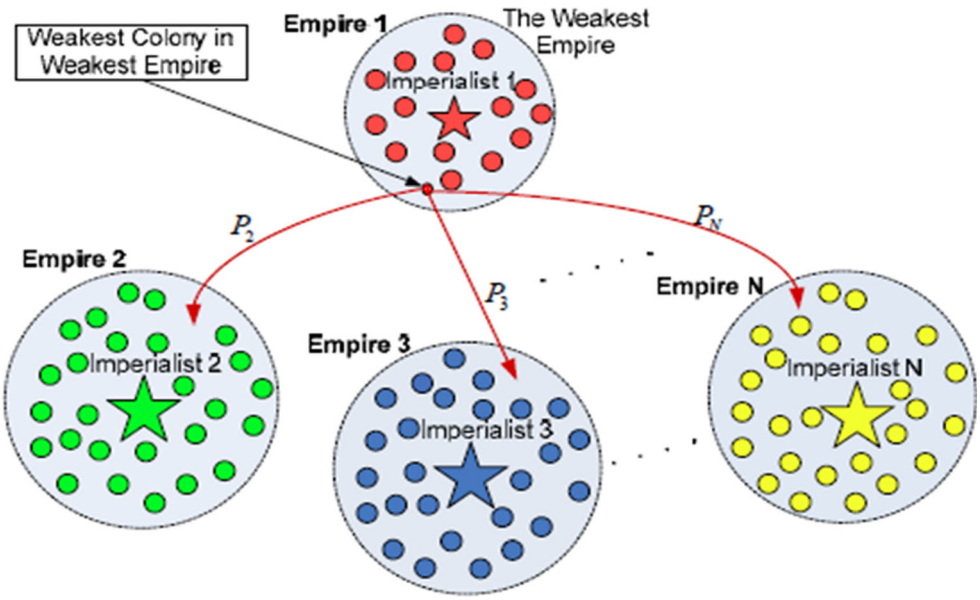

Fig. 4 Colonial competition among several imperialists

Table 3 Details of ICA

(1) The selection of random points in the function and initial valuing of the empire
(2) The colonies movement to the corresponding imperialist country (the policy of assimilation or absorption)
(3) Apply the revolution operator
(4) If a colony is in an empire that has lower cost than that imperialist, change that colony and imperialist positions
(5) Choose the total cost of all the empire (of both the imperial and colonial power)
(6) Select the weakest colony (colonies) from the weakest empire, and give them to the empire that is identical to it (Imperialistic competition)
(7) Remove powerless empires
(8) If there is only one empire then stop, otherwise go to step 2

normalized cost and the possession probability of any empire is defined by Eq. (13):

$$P_{P_n} = \left| \frac{\text{N.T.C.}_n}{\sum_{i=1}^{N_{\text{imp}}} \text{N.T.C.}_i} \right| \tag{13}$$

To divide the colonies among the empires based on their possession probability, vector P is defined by Eq. (14):

$$P = \left[P_{p_1}, P_{p_2}, \ldots, P_{p_{N_{\text{imp}}}} \right] \tag{14}$$

Thereafter, a vector of the same size of P is created as shown in Eq. (15, 16) and its elements are distributed as the same random numbers.

$$R = \left[r_1, r_2, \ldots, r_{N_{imp}} \right] \tag{15}$$

$$r_1, r_2, \ldots, r_{N_{\text{imp}}} \sim U(0,1) \tag{16}$$

Subsequently, vector D by subtracting the vector R from vector P is defined by Eq. (17):

$$\begin{aligned} D = P - R &= \left[D_1, D_2, \ldots, D_{N_{\text{imp}}} \right] \\ &= \left[P_{P_1} - r_1, P_{P_2} - r_2, \ldots, P_{P_{N_{\text{imp}}}} - r_{N_{\text{imp}}} \right] \end{aligned} \tag{17}$$

6. Falling weak empires

Inevitably, during the imperialist competitions, poor empires fall gradually, while stronger empires take their colonies. Different conditions can be considered for the falling of an empire. In the proposed algorithm, an empire is removed when lose its colonies. Table 3 presents the details of the colonial competitive algorithm, as it can be seen that there are 8 steps which are compulsory for running this algorithm.

5 Proposed method

In this study, we focus on the human iris tissue identification by carrying out image preprocessing techniques to achieve the region of interest (ROI) from the individual iris tissue images. Then, we have used GLDM method for feature extraction and finally, we have trained hybrid MLPNN with ICA classifier for classification purpose in order to achieve high accuracy rate in recognizing the human iris tissues.

5.1 GLDM feature extraction

For extracting iris tissue features, we need an efficient feature extraction method to extract the best iris tissue features for our work. So, for this goal, we used GLDM feature extractor.

In this analysis, four possible forms of the vector δ are considered: $(-d, -d)$, $(d, 0)$, $(-d, d)$, and $(0, d)$, in which d is the distance and in this study, we considered its value equal to 11. Five texture features were measured from $D(i|\delta)$ which include: contrast, angular, entropy, mean, and inverse difference moment [27]; in addition, four probability density functions were obtained for the four different displacement vectors with d, and texture features were calculated for each of the probability density function (PDF). This PDF also is computed from four fundamental directions: 0, 45, 90, and 135. Finally, $\Delta x, \Delta y$ are the parameters of the method, and they were set as (1, 1), (2, 2), (5, 5) for our experimental results.

5.2 MLPNN-ICA proposed method

For recognizing and detecting the iris region, a hybrid MLPNN-ICA classifier was performed in this work and the iris tissue images that are preprocessed with a total of 50 people (that are 350 images) were considered as the input layers and 1 neuron was considered as the output layer.

In order to optimize the process of training, the parameters play a crucial role; therefore, we have assessed our proposed technique with miscellaneous parameters that they were set as in Table 4. Then, in order to depict our methods, we have modeled them as shown in Fig. 5. As can be seen in Fig. 5, our proposed method has four fundamental stages, e.g., iris tissue image acquisition (for enrollment and authentication stage), iris tissue image localization, and iris tissue normalization (for

Table 4 Set of parameters for ICA

Number of decades	Number of initial countries (N.I.C)	Number of initial imperialists (N.I.I)	Revolution rate	Assimilation coefficient	Assimilation angle coefficient
10	500	8	0.2	2	0.5
40	200	30	0.3	2	0.5
100	200	30	0.3	2	0.5
100	200	60	0.3	2	0.5
100	200	70	0.5	2	0.5
500	200	70	0.2	2	0.5
1000	200	70	0.2	2	0.5
2000	200	50	0.2	2	0.5

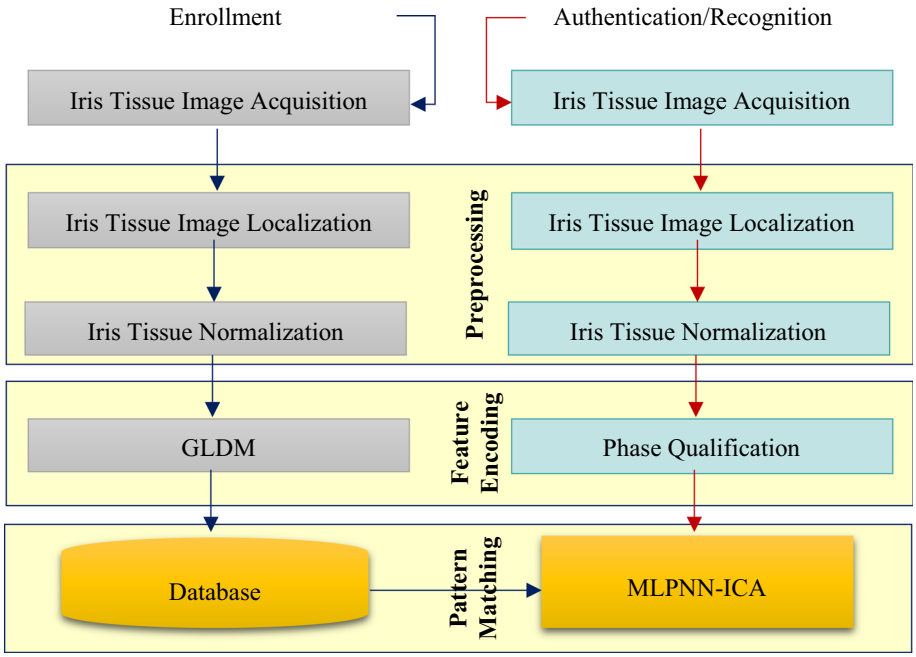

Fig. 5 Proposed block diagram of the iris tissue recognition system

preprocessing stages), GLDM and phase qualification (for feature extraction stage), and hybrid MLPNN-ICA classifier (for pattern matching stage).

6 Experimental results

6.1 CASIA-Iris V3 database and UCI machine learning repository datasets

For analyzing the efficiency of the proposed method, we utilized CASIA-Iris V3 database and three datasets from the UCI machine learning repository. CASIA-Iris V3 database has been provided by the Institute of Automation of the Chinese Academy of Sciences. It includes seven images for each individual and the dimension of iris tissue images are 320 × 280 in JPEG format [31]. Also, in order to evaluate the performance of the proposed method, since we are looking for the most appropriate and standardized machine learning datasets for this purpose, we used the three UCI datasets (breast cancer, iris flowers, and wine). The first dataset has 699 instances and 9 features of breast cancer dataset. The second dataset, iris flowers dataset, has 150 instances with 4 features, and the last one is wine dataset, which has 178 instances with 13 features [32].

6.2 GLDM feature extraction

The iris tissue features were extracted from the normalized iris tissue images using GLDM (the statistical textural feature method). GLDM calculates the GLDM probability density functions (PDF) for the given normalized iris tissue images. The experimental results were carried out for all the 350 iris texture images. The computational time of the proposed method that is required to extract features of 350 iris tissue images (i.e., 50 people and 7 images from each

Table 5 Elapsed time of GLDM feature extraction results of our proposed method

Method	Time (s)
GLDM	29.203610

of them) is shown in Table 5, and we also depicted Fig. 6 in order to demonstrate the GLDM PDF forms of extracted features of the iris tissue images. From the top left graph of Fig. 6, it can be seen that at first from 0 to around 50, it rises sharply from under 2×10^4 to 2.5×10^4, then from about 50–200, it increases slowly from 2×10^4 to above 3×10^4, and finally, it plateaus from 200 to the end of the graph. From the top right graph (PDF form 2) of Fig. 6, it can be seen that the probability density functions from 0 to 200 soar suddenly to above 3×10^4 and it stabilizes ultimately to the end of the graph. From PDF form 3, it is clear that the probability density functions start from 0 to 200 and it escalates from about 2×10^4 to around 3.5×10^4 and finally, from nearly 200 to the end of the graph, it becomes stable. The last graph (PDF form 4) shows the zooming form of PDF form 2. So, from these four graphs, it is clear that although they all have almost the same trends, the last graph which is located in bottom right corner has extracted nearly exact features rather than the rest of the graphs of Fig. 6.

6.3 MLPNN-ICA results

According to the extracted iris tissue features described in prior section, we used these features to train our hybrid MLPNN-ICA classifier in order to distinguish the iris tissue of each individual. For this purpose, 350 layers for the input layer and 100 layers for the hidden layer were considered for our network. Then, our network with ICA was trained accurately and ultimately; it acquired a high percentage of performance.

Table 6 Comparison of results of our proposed method with the other existing methods

Methodology	Accuracy rate %
Liam et al. [33]	64.64
Bansal et al. [12]	87.50
Nabti et al. [34]	88.32
Dhage et al. [35]	90.05
Abhyankar and Schuckers [36]	92.26
Hajari et al. [37]	97.21
Sahmoud and Abuhaiba [38]	98.76
Ahmadi and Akbarizadeh [22]	95.36
Proposed method	99.99

In order to show the efficiency of our proposed method, we performed comparisons among the proposed method and some other existing methods [12, 22, 33–38] on CASIA-Iris V3 and UCI databases. Table 6 shows the accuracy rates among these methods. In Tables 7 and 8, accuracy rates obtained from the proposed method with different parameters on CASIA-Iris V3 and UCI databases are presented. As can be seen, the results in Table 7 show that the current study has adequate efficiency, and the proposed method is proper in order to run low power applications.

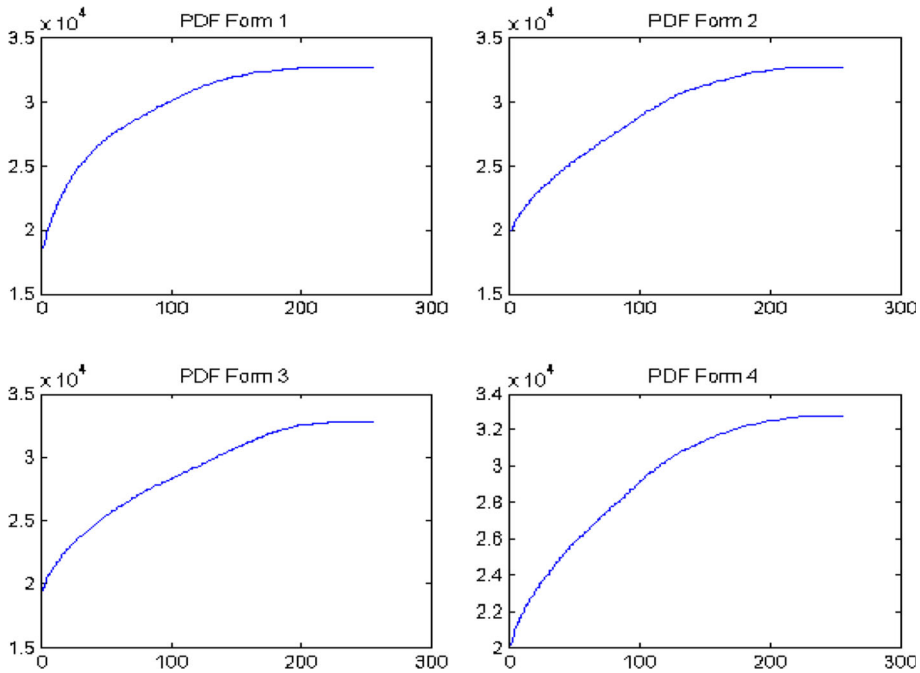

Fig. 6 Four GLDM PDF forms of extracted features of the iris tissue image

Table 7 Results of hybrid MLPNN-ICA classifier on CASIA-Iris V3 dataset

Number of decades	Number of neuron in each layer	Number of initial countries (N.I.C)	Number of initial imperialists (N.I.I)	Revolution rate	Assimilation coefficient	Assimilation angle coefficient	Accuracy rate %	Time (s)
10	5	500	8	0.2	2	0.5	89.71	417.05
40	5	200	30	0.3	2	0.5	91.15	543.76
100	10	200	30	0.3	2	0.5	91.35	1343.5
100	5	200	60	0.3	2	0.5	91.89	1222.8
100	10	200	70	0.5	2	0.5	92.30	1299.8
500	10	200	70	0.2	2	0.5	93.08	5257.4
1000	10	200	70	0.2	2	0.5	93.44	9524.8
2000	10	200	50	0.2	2	0.5	99.99	25,195.2

Table 8 Results of hybrid MLPNN-ICA classifier on UCI datasets

Dataset	Number of decades	Number of neuron in each layer	Number of initial countries (N.I.C)	Number of initial imperialists (N.I.I)	Revolution rate	Assimilation coefficient	Assimilation angle coefficient	Accuracy rate %	Time (s)
Breast cancer	100	10	200	30	0.3	2	0.5	96.88	1549.77
Breast cancer	200	10	200	50	0.3	2	0.5	99.56	2521.50
Iris flowers	100	10	200	30	0.3	2	0.5	98.51	1326.37
Iris flowers	300	10	200	50	0.3	2	0.5	99.66	3228.49
Wine	100	10	200	30	0.3	2	0.5	99.44	1356.98
Wine	300	10	200	50	0.3	2	0.5	99.63	4526.39

Table 7 reports the accuracy rates of the proposed method at several decades (10, 40, 100, 500, 1000 and 2000), different number of neurons in each layer (5 and 10), various number of initial countries (200 and 500), miscellaneous number of initial imperialist (8, 30, 50, 60 and 70), several revolution rates (0.2, 0.3 and 0.5), assimilation coefficient equal to 2, and assimilation angle coefficient equal to 0.5 on CASIA-Iris V3 dataset. In this table, the highest accuracy rate is related to the proposed hybrid MLPNN-ICA classifier that is 99.99% with the following parameter setting: number of initial imperialists equal to 50, number of initial countries equal to 200, number of neuron in each layer equal to 10, and number of decades equal to 2000. This accuracy rate is the best rate

Table 9 Summary of results of our proposed method obtained after 100 independent runs and different parameters

Methods	Objective function value			Standard deviation	Average elapsed time (s)
	Best	Mean	Worst		
MLPNN-ICA	0.0284	− 0.0109	0.3009	0.1685	802.391279

Number of neuron in each layer 10, number of initial countries (N.I.C) 200, number of initial imperialists (N.I.I) 50, revolution rate 0.2, assimilation coefficient 2, assimilation angle coefficient 0.5

Table 10 Summary of results of our proposed method obtained after 500 independent runs and different parameters

Methods	Objective function value			Standard deviation	Average elapsed time (s)
	Best	Mean	Worst		
MLPNN-ICA	0.0182	− 0.0268	0.0782	0.1327	3619.063276

Number of neuron in each layer 10, number of initial countries (N.I.C) 200, number of initial imperialists (N.I.I) 50, revolution rate 0.2, assimilation coefficient 2, assimilation angle coefficient 0.5

Table 11 Summary of results of our proposed method obtained after 1000 independent runs and different parameters

Methods	Objective function value			Standard deviation	Average elapsed time (s)
	Best	Mean	Worst		
MLPNN-ICA	0.0161	− 0.0329	0.0252	0.1229	7466.547162

Number of neuron in each layer 10, number of initial countries (N.I.C) 200, number of initial imperialists (N.I.I) 50, revolution rate 0.2, assimilation coefficient 2, assimilation angle coefficient 0.5

Table 12 Summary of results of our proposed method obtained after 2000 independent runs and different parameters

Methods	Objective function value			Standard deviation	Average elapsed time (s)
	Best	Mean	Worst		
MLPNN-ICA	0.0146	− 0.0273	0.0175	0.1179	14,076.276766

Number of neuron in each layer 10, number of initial countries (N.I.C) 200, number of initial imperialists (N.I.I) 50, revolution rate 0.2, assimilation coefficient 2, assimilation angle coefficient 0.5

and according to our observations, a greater number of neurons in each layer carry out better performance than a lower number of neurons.

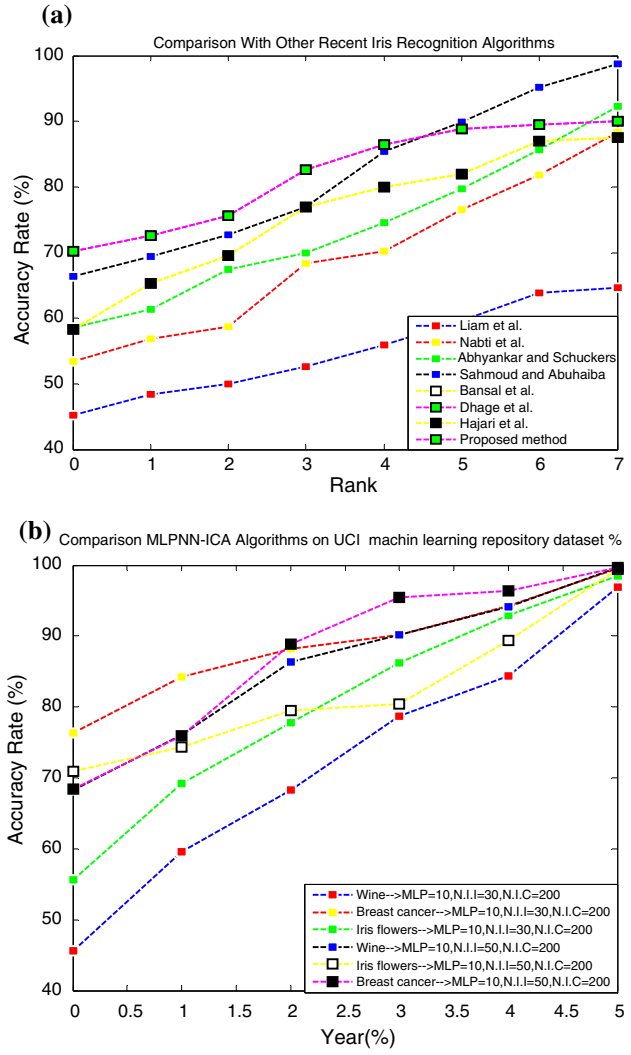

Fig. 7 CMC curve for the comparison our proposed method between CASIA-Iris V3 dataset and UCI datasets. **a** CASIA-Iris V3 dataset. **b** UCI datasets

Table 8 illustrates the accuracy rates for our proposed method at different decades (100, 200 and 300), with 10 neurons in each layer, 200 initial countries, various number of initial imperialists (30 and 50), 0.3 revolution rate, assimilation coefficient equal to 2, and assimilation angle coefficient equal to 0.5 on the UCI machine learning repository datasets for breast cancer, iris flower, and wine. Based on this table, the highest accuracy rate is for wine dataset with 300 decades, 10 neurons in each layer, 200 initial countries, and 50 initial imperialists. This accuracy rate is logically satisfactory and on the basis of our observations, the greater number of initial imperialists gives the perfect results.

In order to demonstrate the robustness of our proposed method, we also tested our algorithm with various parameters and different executing times, e.g., 100, 500, 1000, and 2000; our results are shown in Tables 9, 10, 11, and 12, respectively. Tables 9, 10, 11, and 12 summarize the best, mean and the worst values of the objective function along with its standard deviation and the average elapsed time (s) for different executing times and various parameters. It was observed that among all of these four tables, Table 10 after 500 independent runs has the highest value for the worst. The multifarious parameters in this case were as follows: number of neuron in each layer 10, number of initial countries (N.I.C) 200, number of initial imperialists (N.I.I) 50, revolution rate 0.2, assimilation coefficient 2, and assimilation angle coefficient 0.5. The least values of the objective function (0.0182) and standard deviation (0.1327) were obtained in this case; however, Table 12, with 2000 independent runs and the same parameters, gives the best optimum results. The least value of the objective function (0.0146) and standard deviation (0.1179) is achieved in Table 12.

We further employed CMC which indicates the accuracy rate versus rank to make more comparisons of the proposed method with other existing methods, which is shown in Fig. 7. Figure 7a shows the changes in the

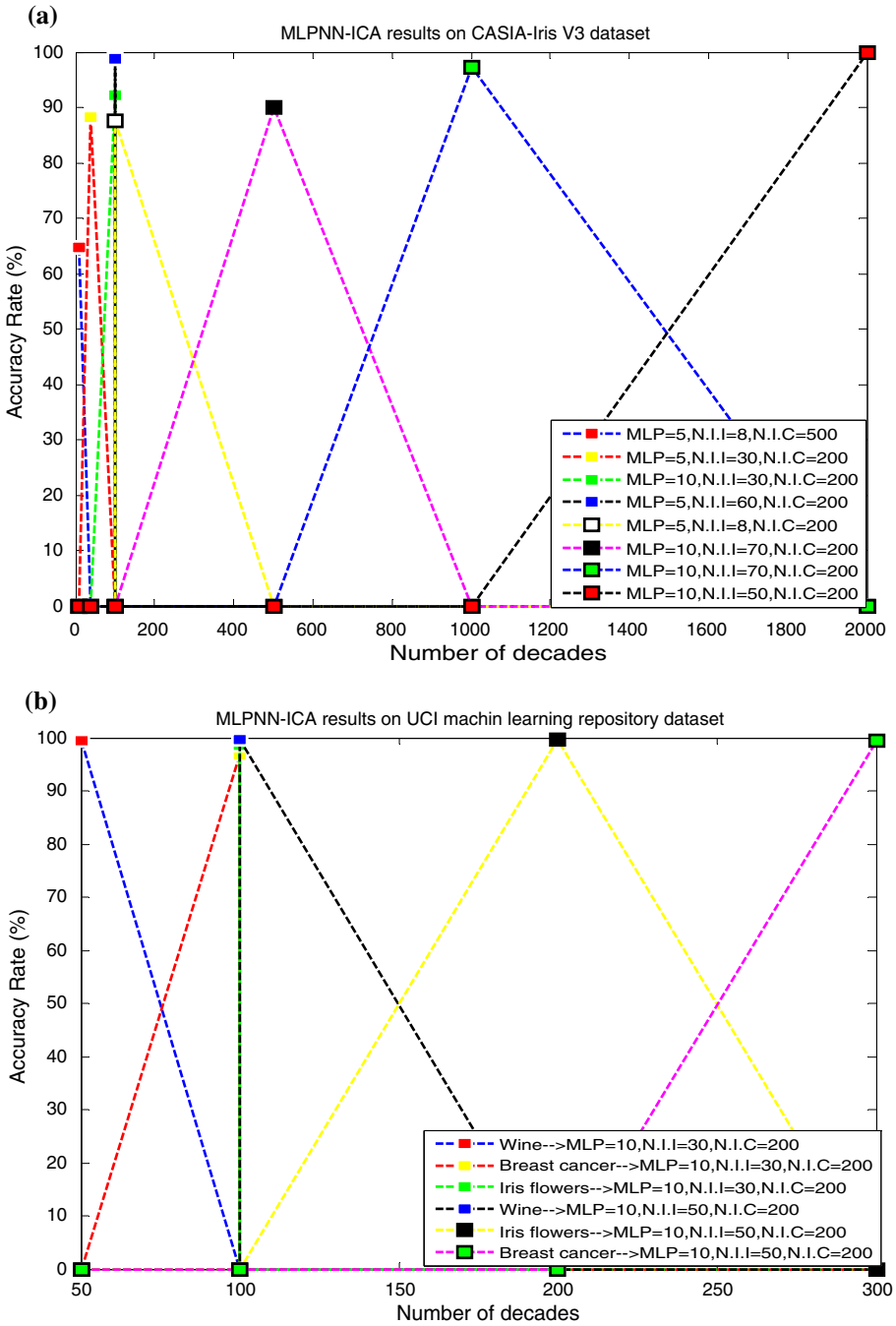

Fig. 8 Results of hybrid MLPNN-ICA classifier. **a** CASIA-Iris V3 dataset, **b** UCI datasets

performance of other methods based on different datasets. Figure 7b demonstrates that our proposed method based on the hybrid MLPNN-ICA classifier has more efficiency based on UCI datasets. Dhage et al. [35] have similar progress with our proposed method until rank 5. It seems that recognition efficiency is related to the noise level in each dataset. Because the low level of noise yielded matching scores among a set of individuals and iris tissue codes with a high percentage of reliability, it produces the most reliable scores. If the level of noise is high, the matching scores are unreliable. By considering the recognition performance trust ability, it is shown that from rank 5–7, our proposed method has the most progress among others. Furthermore, by considering the reliability of recognition performance, it can be seen that the hybrid MLPNN-ICA classifier is more stable, faster, and more reliable.

Moreover, the accuracy rate of our proposed method was compared with different factors on CASIA-Iris V3 and three UCI machine learning repository such as breast

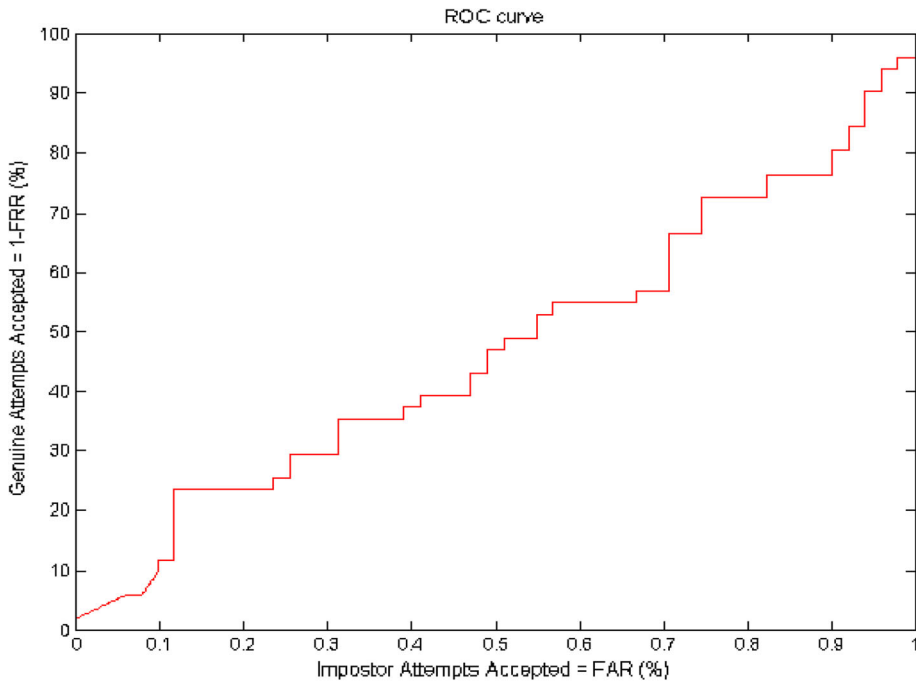

Fig. 9 ROC curve for verification of our proposed method

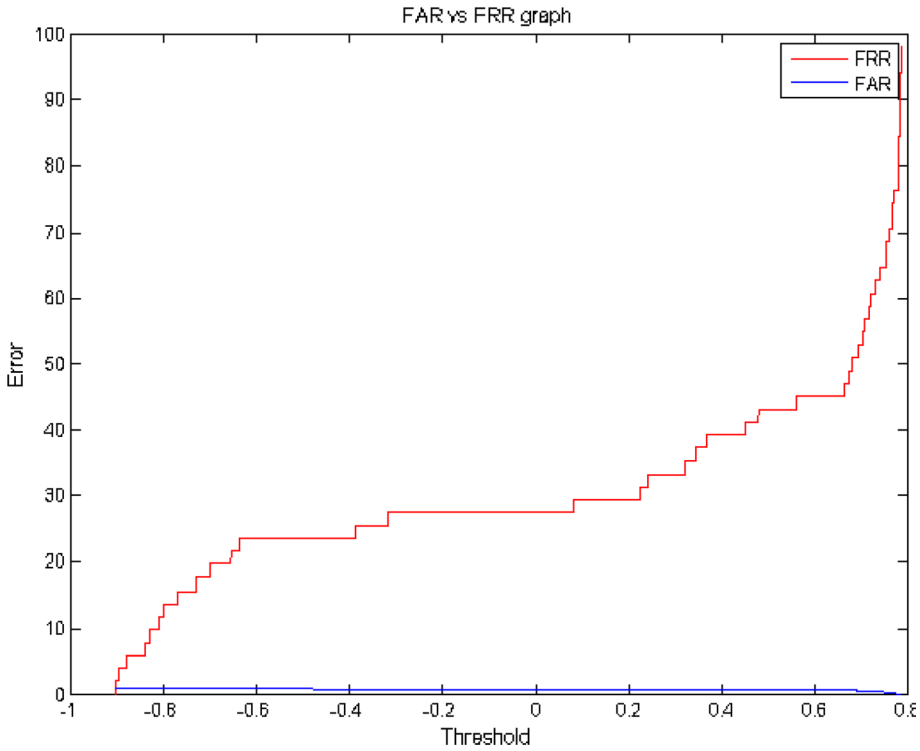

Fig. 10 Equal error rate (EER) of our proposed method

cancer, iris flowers, and wine datasets, respectively. As shown in Fig. 8a, the result of hybrid MLPNN-ICA classifier on CASIA-Iris V3 dataset with 2000 decades, 10 layers in each neuron, 50 initial imperialists, and 200 initial countries, outperforms the other existing parameters. In Fig. 8b, the result on iris flowers of UCI datasets with 300 decades, 10 layers in each neuron, 50 initial imperialists, and 200 initial countries obtained about 99% accuracy rate, which is better efficiency rate among breast cancer and wine datasets. So, our work acquires high level of accuracy rate on both CASIA-Iris V3 and UCI machine learning repositories datasets with different parameters.

When it comes to express the performance of a recognition system based on biometric traits, the best and usual

way is to illustrate at least two things: FAR to FRR correspondence in a ROC curve (preferably in logy coordinate, with EER indicator) and genuine/imposter experimental score distributions (preferably in logy coordinate, to enhance the two) (Figs. 9, 10).

7 Conclusion

In this paper, a new iris tissue recognition approach based on multi-layer perceptron neural network and imperialist competitive algorithm (MLPNN-ICA) was proposed to classify the iris tissue images. The main goals of the paper were defined to improve the accuracy rate of the iris tissue. We applied GLDM for feature extraction step and then, for matching step, we used a combination of MLPNN and ICA classifier.

In the experimental results, we conducted CASIA-Iris V3 database and UCI machine learning repository datasets. Hence, the hybrid MLPNN-ICA classifier is an effective, appropriate, satisfaction, stable, robust, and competitive recognition efficiency for the human iris tissue recognition system, and achieves better experimental outcomes rather than the use of hybrid MLPNN and ICA classifier separately. In addition, we evaluated our proposed method in cases of ROC and CMC to be comparable in relation to the previous works. Our experiments confirmed that the combination of MLPNN and ICA classifier outperforms the previous methods and significantly leads to the improvement in accuracy rate in the human iris recognition system.

Acknowledgements The authors would like to acknowledge the financial support from the Shahid Chamran University of Ahvaz under Grant Number 96/3/02/16670. Appreciation also goes to the anonymous reviewers whose comments helped us to improve the manuscript.

Compliance with ethical standards

Conflict of interest We declare that there are no conflicts of interest regarding the publication of this paper.

References

1. Saba T, Altameem A (2013) Analysis of vision based systems to detect real time goal events in soccer videos. Appl Artif Intell 27:656–667
2. Li C, Zhou W, Yuan S (2015) Iris recognition based on a novel variation of local binary pattern. Vis Comput 31:1419–1429
3. Colores-Vargas JM, García-Vázquez M, Ramírez-Acosta A, Pérez-Meana H, Nakano-Miyatake M (2013) Video images fusion to improve iris recognition accuracy in unconstrained environments. In: Mexican conference on pattern recognition. Springer, Berlin, pp 114–125
4. Rahulkar AD, Waghmare LM, Holambe RS (2014) A new approach to the design of hybrid finer directional wavelet filter bank for iris feature extraction and classification using k-out-of-n: a post-classifier. Pattern Anal Appl 17:529–547
5. Sun Z, Tan T, Wang Y (2004) Robust encoding of local ordinal measures: a general framework of iris recognition. In: International workshop on biometric authentication. Springer, Berlin, pp 270–282
6. Alvarez-Betancourt Y, Garcia-Silvente M (2014) An overview of iris recognition: a bibliometric analysis of the period 2000–2012. Scientometrics 101:2003–2033
7. Kong WK, Zhang D (2001) Accurate iris segmentation based on novel reflection and eyelash detection model. In: Proceedings of 2001 international symposium on intelligent multimedia, video and speech processing: IEEE, pp 263–266
8. Samanta S, Ahmed SS, Salem MAMM, Nath SS, Dey N, Chowdhury SS (2015) Haralick features based automated glaucoma classification using back propagation neural network. In: Proceedings of the 3rd international conference on frontiers of intelligent computing: theory and applications (FICTA) 2014. Springer, Cham, pp 351–358
9. Othman N, Houmani N, Dorizzi B (2015) Quality-based super resolution for degraded iris recognition. In: Pattern recognition applications and methods. Springer International Publishing, pp 285–300
10. Deshmukh M, Prasad MV (2015) Partial segmentation and matching technique for iris recognition. In: Computational intelligence in data mining. Springer India, pp 77–86
11. Khalighi S, Pak F, Tirdad P, Nunes U (2015) Iris recognition using robust localization and non-subsampled contourlet based features. J Signal Process Syst 81:111–128
12. Bansal A, Agarwal R, Sharma RK (2015) Determining diabetes using iris recognition system. Int J Diabetes Dev Ctries 35:432–438
13. Wang N, Li Q, El-Latif AAA, Zhang T, Niu X (2014) Toward accurate localization and high recognition performance for noisy iris images. Multimed Tools Appl 71:1411–1430
14. Wang Y, Tan T, Jain AK (2003) Combining face and iris biometrics for identity verification. In: International conference on audio-and video-based biometric person authentication. Springer, Berlin, pp 805–813
15. Kordjazi N, Rahati S (2012). ait recognition for human identification using ensemble of LVQ neural networks. In: 2012 International conference on biomedical engineering (ICoBE). IEEE, pp 180–185
16. Ahmadi N, Nilashi M (2018) Iris texture recognition based on multilevel 2-D Haar wavelet decomposition and Hamming distance approach. J Soft Comput Decis Support Syst 5(3):16–20
17. Jain YK, Verma MK (2012) Comparison of phase only correlation and neural network for iris recognition. Int J Comput Sci Issues 1:165–171
18. Atashpaz-Gargari E, Lucas C (2007) Imperialist competitive algorithm: an algorithm for optimization inspired by imperialistic competition. In: 2007 IEEE congress on evolutionary computation. IEEE, pp 4661–4667
19. Niknam T, Fard ET, Pourjafarian N, Rousta A (2011) An efficient hybrid algorithm based on modified imperialist competitive algorithm and K-means for data clustering. Eng Appl Artif Intell 24:306–317
20. Qian P, Xi C, Xu M, Jiang Y, Su KH, Wang S, Jr RFM (2018) SSC-EKE: semi-supervised classification with extensive knowledge exploitation. Inf Sci 422:51–76
21. Belkin M, Niyogi P, Sindhwani V (2006) Manifold regularization: a geometric framework for learning from labeled and unlabeled examples. J Mach Learn Res 7:2399–2434
22. Ahmadi N, Akbarizadeh G (2018) Hybrid robust iris recognition approach using iris image pre-processing, two-dimensional gabor

features and multi-layer perceptron neural network/PSO. IET Biom 7(2):153–162
23. Burge M, Burger W (1996) Ear biometrics. In: Jain A, Bolle R, Pankanti S (eds) biometrics. Springer, Boston, pp 273–285
24. Ahmadi N, Akbarizadeh G (2015) Iris recognition system based on canny and LoG edge detection methods. J Soft Comput Decis Support Syst 2(4):26–30
25. Davida GI, Frankel Y, Matt BJ (1998) On enabling secure applications through off-line biometric identification. In: sp. IEEE, p 0148
26. Ahmadi N, Akbarizadeh G (2016) A review of iris recognition based on biometric technologies. Transylv Rev 24(4):151–163
27. Weszka JS, Dyer CR, Rosenfeld A (1976) A comparative study of texture measures for terrain classification. IEEE Trans Syst Man Cybern 4:269–285
28. Graves A, Fernández S, Gomez F, Schmidhuber J (2006) Connectionist temporal classification: labelling unsegmented sequence data with recurrent neural networks. In: Proceedings of the 23rd international conference on Machine learning. ACM, pp 369–376
29. El-Bakry HM (2002) Human Iris detection using fast cooperative modular neural nets and image decomposition. Mach Graph Vis Int J 11(4):499–512
30. Russo A, Raischel F, Lind PG (2013) Air quality prediction using optimal neural networks with stochastic variables. Atmos Environ 79:822–830
31. Database of Human Iris. Institute of Automation of Chinese Academy of Sciences (CASIA). Found on the Web page, http://www.cbsr.ia.ac.cn/english/IristissueDatabase.asp. Accessed 1 June 2017
32. Murphy PM, Aha DW (1994) UCI Repository of machine learning databases. The University of California, Department of Information and Computer Science, Irvine. http://www.ics.uci.edu/∼mlearn/MLRepository.html. Accessed 1 June 2017
33. Liam LW, Chekima A, Fan LC, Dargham JA (2002) Iris recognition using self-organizing neural network. In: Student conference on IEEE research and development. SCOReD 2002, pp 169–172
34. Nabti M, Bouridane A (2008) An effective and fast iris recognition system based on a combined multiscale feature extraction technique. Pattern Recogn 41:868–879
35. Chouhan R, Jha RK, Biswas PK (2012) Wavelet-based contrast enhancement of dark images using dynamic stochastic resonance. In: Proceedings of the 8th Indian conference on computer vision, graphics and image processing. ACM, p 73
36. Abhyankar A, Schuckers S (2010) Novel biorthogonal wavelet based iris recognition for robust biometric system. Int J Comput Theory Eng 2:233
37. Hajari K, Gawande U, Golhar Y (2016) Neural network approach to iris recognition in noisy environment. Procedia Comput Sci 78:675–682
38. Sahmoud SA, Abuhaiba IS (2013) Efficient iris segmentation method in unconstrained environments. Pattern Recogn 46:3174–3185